Peer-reviewed version available at Electronics 2019, 8, 167; doi:10.3390/electronics8020167

Article

Multi-Points Cooperative Relay in NOMA System with *N-1* DF Relaying Nodes in HD/FD mode for *N* User Equipments with Energy Harvesting

Thanh-Nam Tran [1,†,‡], and Miroslav Voznak [2,†]

[1] Email: thanh.nam.tran.st@vsb.cz
[2] Email: miroslav.voznak@vsb.cz
† Faculty of Electrical Engineering and Computer Science, Technical University of Ostrava, 17. listopadu 2172/15, 708 33 Ostrava-Poruba, Czech Republic;
‡ Faculty of Electronics and Telecommunications, Sai Gon University, 220 Tran Binh Trong st., Dict. 5, Hochiminh city, Vietnam.

Abstract: Non-Orthogonal Multiple Access (NOMA) is the key technology promised to be applied in next-generation networks in the near future. In this study, we propose a multi-points cooperative relaying (MPCR) NOMA model instead of just using a relay as the previous studies. Based on the channel state information (CSI), the base station (BS) selects a closest user equipment (UE) and sends a superposed signal to this UE as a first relay node. We have assumed that there are *N* UEs in the network and N*th* UE, which is farthest from BS, has the poorest quality signal transmitted from the BS compared other UEs. N*th* UE received the forwarded signal from *N-1* relaying nodes that are UEs with better signal quality. At the i*th* relaying node, it detect its own symbol by using successive interference cancellation (SIC) and will forward the composite signal to the next closest user, namely i+1*th* UE, and include an excess power which will use for energy harvesting (EH) intention at the next UE. By these, the farthest UE in network can be significantly improved. In addition, closed-form expressions of outage probability for users over both the Rayleigh and Nakagami-m fading channels are also presented. Analysis and simulation results performed by Matlab software which are presented accurately and clearly show that the effectiveness of our proposed model and this model consistents with the multi-access wireless network in future.

Keywords: Cooperative NOMA; multi-points DF relaying nodes; half-duplex; full-duplex; Rayleigh fading channels; Nakagami-*m* fading channels; energy harvesting

1. Introduction

The next-generation network (5G) technology has the advantage of increasing system capacity by superior sharing-spectrum efficiency [1]. Therefore, multiple users in the network can be served in the same frequency band/time slot and various allocation power coefficients by the key technology is called Non-Orthogonal Multiple Access (NOMA). The is fundamentally different from previous orthogonal access methods, e.g., Orthogonal Multiple Access (OMA) [2]. In NOMA system, the users with better channels conditions are allocated less transmitting power coefficients. On another hand, the users with worse channels conditions are allocated more transmitting power coefficients to guarantee the quality of service for all users in the system. After receiving a superposed signal, successive interference cancellation (SIC) is done at the end users. In [3], the authors investigated the impact of imperfect SIC on the analysis performance of NONA system. Their analysis results showed that even SIC is not perfect, the performance of the NOMA system is still better than the orthogonal system. A down-link NOMA wireless network was studied in [4] by considering to use a relay for forwarding signals to combat the fading effect of the transmission channel. Authors applied to dual-hop relaying systems with decode-and-forward (DF) or amplify-and-forward (AF) protocols [5]. Relay full-duplex (FD) model over the Rayleigh fading channels using the DF protocol was

investigated the performance by optimizing the transmit power factor [6]. The study impacts of relay selection of cooperative NOMA on the performance system [7]. the authors in [8] proposed a novel best cooperative mechanism (BCM) for wireless energy harvesting and spectrum sharing in 5G network. The [9]-[11] include amplify-and-forward (AF) and decode-and-forward (DF) relaying. In [11], it showed that a dual-hop power line communication (PLC) system can improve the system capacity compared to direct-link (DL) transmission. And M. Rabie et. al. [12] proposed using Multi-hop relay instead of use one hop relay or dual-hop relays. This study, the authors investigated the energy efficiency over PLC channels with assuming log-normal fading. The studies [13] and [14] analyzed the system performance of multi-hop AF/DF relaying over PLC channels in terms of average bit error and ergodic capacity. These studies showed that the system performance can be improve by increasing the number of relaying. In addition, The authors in [15] studied the impact of relay selection (RS) on system performance. The compared results on two-stage versus max-min RS showed that cooperative NOMA system over Rayleigh fading channels with two-stage RS is better than max-min one. We hypothesized that there are N users with the Nth user at the far end from BS with the worst channel condition. The QoS of the Nth user can be improved with the N-1 user's cooperation instead of just receiving a relay cooperation. At each node perform the best neighbor selection to forward the signal next neighbor. The best selection of neighbors is repeated until the signal reaches the destination

In addition, we also consider energy harvesting at UEs. The explosion of the number of wireless devices, radio frequency (RF) energy harvesting becomes a potential technology to convert the energy of receiving wireless signal into electricity. Therefore, the MPCR is not only transmitting information but also delivering energy to the users. In Ref. [16]-[18], there are only users located close BS can collect energy. Because signal reception and energy collection can not be done simultaneously. Thus, the users need to divide the received signal for EH and information decoding (ID) by using power splitting (PS) or time switching (TS) which was called "received TS" [19] and [20]. Though the PS approach has been shown to mostly outperform the receive-TS approach, however, the PS is complicated and inefficient for practical implementation. The research results have shown that PS is better than TS, however, PS is more complex and difficult to practical application than TS. In our study, we consider on compressing both information and energy in one transmission phase instead of splitting it into two transmission phases as the previous studies. And a user faraway from BS can still receive information and collect energy from the nearest relay node. See our model in Fig. 1 for more detail.

In this study we focus on MPCR in NOMA network to improve the quality of service (QoS) for the user faraway form BS with poor signal. In terms of contributions in our research, our main contributions include:

- The first, we propose a down-link side NOMA network with random N UEs.
- The next, we propose a method to improve QoS for farthest distance Nth UE from BS by using $N-1$ UEs as DF relaying nodes in HD or FD modes. UE_i relaying node receives and forwards a superposed signal to next hop which is nearest from UE_i, namely UE_{i+1}. This work will loop until the superposed signal is sent to last UE, namely UE_N.
- A algorithm for selecting relay nodes in MPCR is also presented clearly in next section.
- At UE_i with $i > 1$, the received signal has an excess power is used for energy harvesting to charge the battery with assuming unlimited capacity of the battery.
- In additional, we investigate and find an outage probability and system throughput for each UE, which are written in closed-form expressions.
- Further, The analysis and simulation results are presented in a clear way by the Monte Carlo simulation (10^6 samples of channels) from the Matlab software to prove our propositions.

This article is presented as follows. In next section, namely Experimental Models, we propose models and analysis two transmission scenarios which are called $N-1$ relaying nodes in HD or FD modes. In third section, we have analyzed the system's performance on outage probability and system throughput. In section number IV, we use Matlab software to simulate and results will be

also presented in this section. A summary of the results of our study would be presented in section V, namely Conclusion. End of introducing section.

Notice: In our study, we use a few notations included as

- $h_{a,b}$ is a channel from source a to destination b.
- α_i is an allocation power coefficient for ith UE.
- y_i^{Ω} is the received signal at ith UE with Ω protocol.
- $\gamma_{i\rightarrow x_j}^{\Omega}$ is a signal-to-interference-plus-noise-ratios (SINRs) at ith UE while ith UE decodes x_j symbol.
- $\Pr\{.\}$ is a probability.
- Θ_i^{Ω} is a outage probability of ith UE with Ω protocol over $\Re$ or $\aleph$ which is Rayleigh or Nakagami-m fading channels, respectively.
- R_i^* is a bit rate threshold of ith UE.

2. Experimental Models

In previous studies about NOMA, a direct down-link scenario is considered to serve a number of users in the same time slot. However, in such studies, they are usually fixed number of users. Therefore, they have not shown the generality of the model. In order to ensure the generality, we have upgraded the model to a random and unpredictable number of users.

2.1. Direct link scenario

Based on proposed model in Fig. 1, the BS send a superposed signal to all UEs in the same time slot as expressed

$$S = \sqrt{P_0}\sum_{j=1}^{N}\sqrt{\alpha_j}x_j, \tag{1}$$

Thus, the received signal at all UEs would be expressed as

$$y_i^{Dir} = h_{0,i}\sqrt{P_0}\sum_{j=1}^{N}\sqrt{\alpha_j}x_j + n_i, \tag{2}$$

where $h_{0,i}$, with $i = \{1, N\}$, is denoted as the fading channels from BS to each UE over Rayleigh fading or Nakagami-m fading. And, N is the random number of UEs joined to network, α_j in rule with $\sum_{j=1}^{N}\alpha_j = 1$ is allocation power coefficient for each UE and P_0 is the transmission power of BS. n_i is denoted the additive white Gaussian noise (AWGN) of ith UE, $i = \{1, N\}$, where $n_i \sim CN(0, N_0)$ with zero mean and variance N_0.

It is important to notice that the channel coefficient from BS to each UE, in paired, is expressed as $h_{0,i}$ in our expressions.

In our model, the first user in the nearest distance from the BS with the strongest signal quality was ordered first in the channel gain list. And the list is in decreasing order as follows

$$|h_{0,1}| > |h_{0,2}| > ... > |h_{0,i}| > ... > |h_{0,N-1}| > |h_{0,N}| \tag{3}$$

According to the NOMA theory, users with the worst signal quality should be given priority to allocate the highest transmitting power factor. Another assumption that does not affect the NOMA characteristics, we have assumed that the BS already owns the channel state information (CSI) of all UEs fully. Therefore, the list of allocation power factors is arranged in descending order for each UE in the network as

$$\alpha_1 < \alpha_2 < ... < \alpha_i < ... < \alpha_{N-1} < \alpha_N. \tag{4}$$

Preprints (www.preprints.org) | NOT PEER-REVIEWED | Posted: 10 December 2018 doi:10.20944/preprints201812.0109.v1

Peer-reviewed version available at Electronics 2019, 8, 167; doi:10.3390/electronics8020167

Signals are sent to users from BS in the same power domain with hoping of improving service quality and fairness among users on a near-by-far rule. In Fig. 1, because the x_N symbol has the strongest allocation power factor. Therefore, x_N symbol will be first decoded at all UEs in the network by applying successive interference cancellation (SIC) [20]. And the order of decoding is done sequentially according to the reversed list of power factor allocations presented in (4) expression. The Signal-to-interference-plus-noise ratios (SINRs) of all UEs have been expressed as

$$\gamma_{i\to x_j}^{Dir} = \frac{|h_{0,i}|^2 \rho_0 \alpha_j}{|h_{0,i}|^2 \rho_0 \sum_{k=1}^{j-1} \alpha_k + 1}, \tag{5}$$

where $i = \{2, N\}$ and $j = \{N, i\}$.

In a special case at 1st UE, after it decoded x_j symbols with $j = \{N, 2\}$ by using (5), UE_1 decodes its own symbol x_1 with only self-interference n_1 as

$$\gamma_{1\to x_1}^{Dir} = |h_{0,1}|^2 \rho_0 \alpha_1. \tag{6}$$

And ρ_0 in (5) or (6) is signal-to-noise ratio (SNR) which can be calculated by

$$\rho_i = \frac{P_i}{N_0}, \tag{7}$$

where $i = \{0, N-1\}$, e.g., $\rho_0 = P_0/N_0$ with P_0 is the transmitting power of BS.

The instantaneous bit rate of each UE is showed by

$$R_{i\to x_j}^{Dir} = \frac{1}{2}\log_2\left(1 + \gamma_{i\to x_j}^{Dir}\right), \tag{8}$$

where $i = \{1, N\}$ and $j = \{N, i\}$.

2.2. $N-1$ *DF relaying nodes scenario*

On another hand, system model in [12] has only one relaying to improve the QoS of UEs which are faraway from the BS. We propose a improved model with using a MPCR model instead of using only one user as a relay device. See on Fig. 1, there are N users in the network with descending order channel conditions with N*th* UE has the poorest signal compared to the other UEs

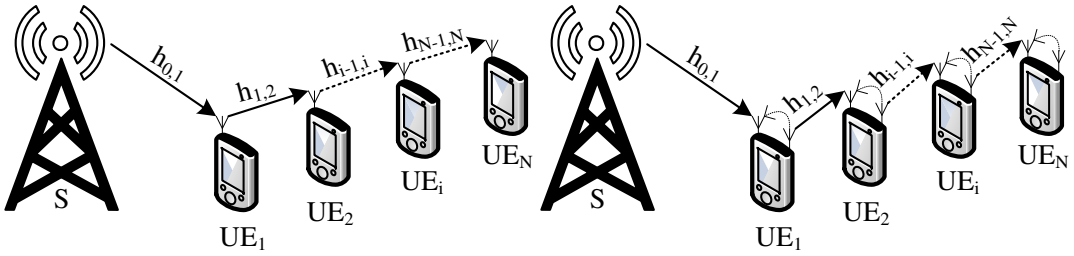

(a) DF relaying nodes in HD mode. (b) DF relaying nodes in FD mode.

Figure 1. The NOMA system with $N-1$ relaying nodes in HD/FD modes.

The authors in [15] proposed the relay selection method to choice the best relay with the best channel condition by using *two-stage relay selection* protocol which outperforms versus *max-min relay selection* protocol. There is a difference compared model in [15] versus our model. The author in [15] selected a best relay in N relays to serve for two other users. In our proposed model Fig. 1, all of $N-1$

UEs can be selected for relaying node. A selected relay nodes set is initialized empty $\varpi = \emptyset$, and a first relaying node can be selected by

$$\varpi_1 = \max \left\{ R^{\Omega}_{i \to x_1} > R^{*}_{1} \right\}, \tag{9}$$

where $R_{i \to x_1}$ is given by (22), and ϖ_1 has been added into $\varpi = \varpi \cup \varpi_1$ then.

BS sends a superposed signal to the closest distance user with strongest channel condition, namely UE_1 in the Fig. 1(a) and 1(b), after BS selected UE_1 as a relay successfully. It is important to point out the difference. In this study, at each relay node has a single or a twin antenna and woks in HD or FD mode.

The received signals at UE_1 in HD or FD modes are respectively the same like (2) or (10) as

$$y_1^{FD} = h_{0,1}\sqrt{P_0}\sum_{j=1}^{N}\sqrt{\alpha_j}x_j + h_{LI,1}\sqrt{P_0}\tilde{x}_1 + n_1, \tag{10}$$

where $h_{LI,1}$ is the interference channel generated by the itself transmitter antenna, and n_1 is the intrinsic noise of the device UE_1.

In case of the UE_1 is working in HD relaying mode, UE_1 decodes its own symbol by applying (5) and (6), respectively. On another hand, the UE_1 is working in FD relaying mode, UE_1 decodes x_j symbol with $j \triangleq \{N, 2\}$ or $j \triangleq 1$ by applying SINRs in (11a) or (11b), respectively,

$$\gamma^{FD}_{1 \to x_j} \triangleq \frac{|h_{0,1}|^2 \rho_0 \alpha_j}{|h_{0,1}|^2 \rho_0 \sum\limits_{k=1}^{j-1} \alpha_{UE_k} + |h_{LI,1}|^2 \rho_1 + 1} \tag{11a}$$

$$\triangleq \frac{|h_{0,1}|^2 \rho_0 \alpha_1}{|h_{LI,1}|^2 \rho_1 + 1}. \tag{11b}$$

Then, UE_1 sends a mixed signal, namely S_1 in (13), to next UE which is next nearest relay node, namely UE_2. The second relay node can be selected by applying (9) as

$$\varpi_2 = \max \left\{ R^{\Omega}_{i \to x_2} > R^{*}_{2}, i = \{1, N\}, i \notin \varpi \right\}, \tag{12}$$

where R^{Ω}_{i} is also given by (22) and not being contained in ϖ which is a selected relay nodes set. We removed UE_i with $i \subset \varpi$ from the relay selection because the signal could be sent back to the previous relay node and the superposed signal is unable send to UE_N. And, the ϖ_2 is also added into ϖ then. Note that the nearest neighbor represented in [25] and [26] are neighbors closest to the BS. However, the authors in [22] have extended the definition of nearest neighbor as the device can set up the transmission channel in the best condition compared to other devices.

A mixed signal is sent to the next relay node as expressed

$$S_1 = \sqrt{P_1}\left(\sqrt{\alpha_1}x_{\emptyset} + \sum_{j=2}^{N}\sqrt{\alpha_j}x_j\right), \tag{13}$$

where $x_{\emptyset}$ is a empty symbol which was also namely x_1 decoded at UE_1.

The received signals at UE_2 in both HD and FD relaying modes are expressed as, respectively,

$$y_2^{HD} = h_{1,2}\sqrt{P_1}\left(\sqrt{\alpha_1}x_{\emptyset} + \sum_{j=2}^{N}\sqrt{\alpha_j}x_j\right) + n_2, \tag{14}$$

and

$$y_2^{FD} = h_{1,2}\sqrt{P_1}\left(\sqrt{\alpha_1}x_\varnothing + \sum_{j=2}^{N}\sqrt{\alpha_j}x_j\right) + h_{LI,2}\sqrt{P_2}\tilde{x}_2 + n_2, \tag{15}$$

where $h_{1,2}$ is the channel from UE_1 to UE_2, P_1 is denoted as transmitting power at UE_1, and $h_{LI,2}$ is loop interference channel from transmitting antenna to receiving one at UE_2. Specially, the x_1 symbol existed in (2) and (10) but it was replaced by $x_\varnothing$ in (14) and (15). Because x_1 was previously decoded and removed from the mixed signal by U_1. Therefore, the power portion α_1 of the $x_\varnothing$ symbol does not contain information and becomes redundant in the mixed signal. We will use this excess power for energy harvesting purposes as describing in the next section

The SINRs for decoding x_j symbol $j \triangleq \{N, 3\}$ and its own symbol, namely x_2 with $j \triangleq 2$, at UE_2 in both HD and FD relaying modes can be expressed as, respectively,

$$\gamma_{2\to x_j}^{HD} \triangleq \frac{|h_{1,2}|^2\rho_1\alpha_j}{|h_{1,2}|^2\rho_1\sum_{k=2}^{j-1}\alpha_k + 1} \tag{16a}$$

$$\triangleq |h_{1,2}|^2\rho_1\alpha_2, \tag{16b}$$

and

$$\gamma_{2\to x_j}^{FD} \triangleq \frac{|h_{1,2}|^2\rho_1\alpha_j}{|h_{1,2}|^2\rho_1\sum_{k=2}^{j-1}\alpha_k + |h_{LI,2}|^2\rho_2 + 1} \tag{17a}$$

$$\triangleq \frac{|h_{1,2}|^2\rho_1\alpha_2}{|h_{LI,2}|^2\rho_2 + 1}, \tag{17b}$$

where (16a) and (17a) with $j \triangleq \{N, 3\}$. Or (16b) and (17b) with $j \triangleq 2$.

After UE_2 decoded its own symbol, it selects a next relay node and sends a new superposed signal to next nearest UE, namely UE_3. This work will loop until a superposed signal sent to farthest UE, namely UE_N in Fig. 1.

Proposed 1: In our study, we propose a energy harvesting model to use excess power in the mixed signals for purposing energy harvesting as Fig. 2. As expressing in (18) and (19), the received signals at i*th* UE, where $i = \{2, N\}$, have an empty $x_\varnothing$ symbol with no information. Thus, the transmit power coefficients of each empty symbol can be harvested. In previous studies, the power for energy harvesting was transmitted to users on different time slots or on different antennas on the receivers. But in this study, we use only one antenna for receiving both signals and energy from the transmitter.

In generally, the received signals at UE_i in both HD and FD relaying nodes can be rewritten by, respectively

$$y_i^{HD} = h_{i-1,i}\sqrt{P_{i-1}}\left(\sum_{l=1}^{i-1}\sqrt{\alpha_l}x_\varnothing + \sum_{k=i}^{N}\sqrt{\alpha_k}x_k\right) + n_i, \tag{18}$$

and

$$y_i^{FD} = h_{i-1,i}\sqrt{P_{i-1}}\left(\sum_{l=1}^{i-1}\sqrt{\alpha_l}x_\varnothing + \sum_{k=i}^{N}\sqrt{\alpha_k}x_k\right) + h_{LI,i}\sqrt{P_i}\tilde{x}_i + n_i, \tag{19}$$

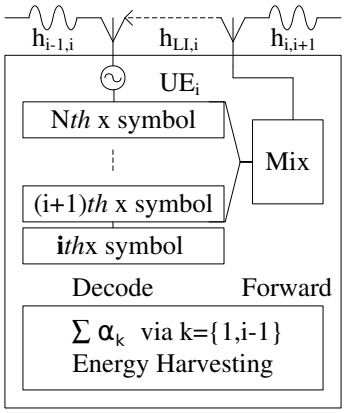

Figure 2. DF protocol and EH protocol at i*th UE* node.

where y_i^{HD} and y_i^{FD} are denoted as receiving signals at UE_i node, $h_{i-1,i}$ is the channels from previous node to current node, P_{i-1} and P_i are transmitting power of previous UE and current UE, respectively. It is important to notice that $\sum_{l=1}^{i-1} \alpha_l + \sum_{k=i}^{N} \alpha_k = 1$.

The SINRs of each i*th* UE relaying node for detecting x_j symbol in HD and FD modes are expressed as, respectively

$$\gamma_{i\to x_j}^{HD} \triangleq \frac{|h_{i-1,i}|^2 \rho_{i-1} \alpha_j}{|h_{i-1,i}|^2 \rho_{i-1} \sum_{k=i}^{j-1} \alpha_k + 1}, \tag{20a}$$

$$\triangleq |h_{i-1,i}|^2 \rho_{i-1} \alpha_j = |h_{0,1}|^2 \rho_0 \alpha_1, \tag{20b}$$

and

$$\gamma_{i\to x_j}^{FD} \triangleq \frac{|h_{i-1,i}|^2 \rho_{i-1} \alpha_j}{|h_{i-1,i}|^2 \rho_{i-1} \sum_{k=i}^{j-1} \alpha_k + |h_{LI,i}|^2 \rho_i + 1}, \tag{21a}$$

$$\triangleq \frac{|h_{i-1,i}|^2 \rho_{i-1} \alpha_j}{|h_{LI,i}|^2 \rho_i + 1} = \frac{|h_{0,1}|^2 \rho_0 \alpha_1}{|h_{LI,1}|^2 \rho_1 + 1}, \tag{21b}$$

where (20a), (21a) with $i \triangleq \{2, N\}$ and $j \triangleq \{N, i\}$. And (20b) and (21b) with $i \triangleq j \triangleq 1$.

In NOMA theory, reachable instantaneous bit rate can be calculated by

$$R_{i\to x_j}^{\Omega} = \frac{1}{2} \log_2 \left(1 + \gamma_{i\to x_j}^{\Omega}\right), \tag{22}$$

where $\Omega = \{HD, FD\}$, $i = \{1, N\}$ and $j = \{N, i\}$.

A selected relay node can be performed by

$$\varpi_i = \max \left\{ R_{i\to x_j}^{\Omega} > R_j^*, i = \{1, N\}, i \notin \varpi \right\}. \tag{23}$$

And, a selected relay node set ϖ after the signal has been sent to the UE_N included

$$\varpi = \varpi_1 \cup \varpi_2 \cup ... \cup \varpi_{N-1} \tag{24}$$

3. The System Performance Analysis

In this section, we evaluate the performance of the system that we have proposed based on outage probability and system throughput, in order.

3.1. Outage Probability

in terms of investigating outage probability, the outage probability is defined as the occurrence of the stop transmitting event if any instantaneous bit rate in (8) or (22) can not reach minimum bit rate thresholds.

The probability density function (PDf) and cumulative distribution function (CDF) of Rayleigh distribution are showed by, respectively,

$$f_{\left|h_{a,b}\right|^2}(x) = \frac{1}{\sigma_{a,b}^2} e^{-\frac{x}{\sigma_{a,b}^2}} dx, \tag{25}$$

and

$$F_{\left|h_{a,b}\right|^2}(x) = 1 - e^{-\frac{x}{\sigma_{a,b}^2}}, \tag{26}$$

where $\left|h_{a,b}\right|^2$ are random independent variables namely x in PDF and CDF, respectively, with a and b are source and destination of channels, and $\sigma_{a,b}^2$ is mean of channel $\left|h_{a,b}\right|^2$.

In generally, the PDF and CDF over nakagami-m fading channels can be expressed, respectively,

$$f_{\left|h_{a,b}\right|^2}(x) = \left(\frac{m}{\sigma_{a,b}^2}\right)^m \frac{x^{m-1}}{\Gamma(m)} e^{-\frac{mx}{\sigma_{a,b}^2}}, \tag{27}$$

and

$$\begin{aligned} F_{\left|h_{a,b}\right|^2}(x) &= \frac{\gamma\left(m, \frac{mx}{\sigma_{a,b}^2}\right)}{\Gamma(m)} \\ &= 1 - e^{-\frac{mx}{\sigma_{a,b}^2}} \sum_{j=0}^{m-1} \left(\frac{mx}{\sigma_{a,b}^2}\right)^j \frac{1}{j!}. \end{aligned} \tag{28}$$

In direct link scenario, outage event occurs if UE_i, where $i = \{1, N\}$, can not decode x_j, where $j = \{N, i\}$. the outage probability for each of joining UE in NOMA system is expressed as

$$\Theta_i^{Dir} = 1 - \prod_{j=N}^{i} \Pr\left(R_{i\to x_j}^{Dir} > R_j^*\right). \tag{29}$$

where $R_{i\to x_j}^{Dir}$ is given by (8) and R_j^* is bit rate threshold of UE_j.

By applying the CDF in (25) and (27), the (29) is solved and it can be rewritten in closed-form as

$$\Re\Theta_i^{Dir} = 1 - \prod_{j=N}^{i} e^{-\frac{R_j^{**}}{\chi_j \rho_0 \sigma_{0,i}^2}}, \tag{30}$$

and

$$\aleph\Theta_i^{Dir} = 1 - \prod_{j=N}^{i} \left[\frac{\left(\frac{m}{\sigma_{0,i}^2}\right)^m \left(\left(\frac{m}{\sigma_{0,i}^2}\right)^{-m} \Gamma(m) + \left(\frac{R_j^{**}}{\chi_j \rho_0}\right)^m \left(\frac{mR_j^{**}}{\chi_j \rho_0 \sigma_{0,i}^2}\right)^{-m} \left(\Gamma\left(m, \frac{mR_j^{**}}{\chi_j \rho_0 \sigma_{0,i}^2}\right) - \Gamma(m) \right) \right)}{\Gamma(m)} \right], \tag{31}$$

where $\Gamma(.)$ and $\Gamma(.,.)$ are gamma and Gamma incomplete functions, $R_j^{**} = 2^{2R_j^*} - 1$. It is important to notice that (30) and (31) are with the users over Rayleigh and Nakagami-m fading channels, respectively. And, χ_j in the (30) and (31) is given by

$$\begin{cases} \chi_j \triangleq \alpha_j - R_j^{**} \sum_{k=1}^{j-1} \alpha_k \\ \chi_j \triangleq \alpha_1 \end{cases} \tag{32}$$

with $j \triangleq \{2, N\}$ or $j \triangleq i$.

Remark 1: Based on our proposed mode with $N-1$ relaying nodes as Fig. 1, we investigate the outage probabilities of number of N UE nodes in both HD and FD modes as

$$\Theta_i^{\Omega} = \left(1 - \underbrace{\prod_{l=1}^{i-1} \Pr\left(R_{l\to x_i}^{\Omega} > R_i^*\right)}_{\eta}\right) \text{ and } \left(1 - \underbrace{\prod_{j=N}^{i} \Pr\left(R_{i\to x_j}^{\Omega} > R_j^*\right)}_{\mu}\right), \tag{33}$$

where η is the successful probability to detect x_i symbol at previous UEs and μ is the successful probability to detect x_j symbol at ith UE. In a special case of ith UE with $i = 1$, It is important to notice that η in (33) is equal with zero and the (33) becomes the same with (29). In (33), η and μ are also solved by applying the CDF and gotten closed-form outage probability of each UE node over Rayleigh fading channel on both HD and FD modes as, respectively,

$$\Re\Theta_i^{HD} = \underbrace{\left(1 - \underbrace{\prod_{l=1}^{i-1} e^{-\frac{R_i^{**}}{\psi_i \rho_{l-1} \sigma_{l-1,l}^2}}}_{\eta}\right)}_{A_1} \underbrace{\left(1 - \underbrace{\prod_{j=N}^{i} e^{-\frac{R_j^{**}}{\chi_j \rho_i \sigma_{i-1,i}^2}}}_{\mu}\right)}_{A_2}, \tag{34}$$

and

$$\Re\Theta_i^{FD} = \underbrace{\left(1 - \underbrace{\prod_{l=1}^{i-1} \left(e^{-\frac{R_i^{**}}{\psi_i \rho_{l-1} \sigma_{l-1,l}^2}} \frac{\psi_i \rho_{l-1} \sigma_{l-1,l}^2}{\psi_i \rho_{l-1} \sigma_{l-1,l}^2 + R_i^{**} \rho_l \sigma_{h_{LI,l}}^2}\right)}_{\eta}\right)}_{B_1}$$
$$\underbrace{\left(1 - \underbrace{\prod_{j=N}^{i} \left(e^{-\frac{R_j^{**}}{\chi_j \rho_{i-1} \sigma_{i-1,i}^2}} \frac{\chi_j \rho_{i-1} \sigma_{i-1,i}^2}{\chi_j \rho_{i-1} \sigma_{i-1,i}^2 + R_j^{**} \rho_i \sigma_{LI,i}^2}\right)}_{\mu}\right)}_{B_2}. \tag{35}$$

To be clearer, here are some information that should be clearly explained. We denoted $\Re\Theta_i^{\Omega}$, where $i = \{1, N\}$ and $\Omega = \{HD, FD\}$, is the outage probability of UE_i over Rayleigh fading channels. The η symbol in both (34) and (35) is the successful detected x_i symbol at UE_l probability with $l = \{1, i-1\}$. Similarly, the μ symbol in both (34) and (35) is the successful detected x_j symbol at UE_i. Here are two cases such as:

- First case with $i = 1$, $\eta = 0$ in both (34) and (35) then. And, the outage probability of UE_1 in HD/FD mode is $\Re\Theta_i^{\Omega} = \{A_2, B_2\}$.
- And second case with $i > 1$, the (34) and (35) are with $\Re\Theta_i^{\Omega} = \{A_1.B_1, A_2.B_2\}$.

In only the second case: ψ_i in both (34) and (35) is given by

$$\Psi_i = \left(\alpha_i - R_i^{**}\sum_{k=l}^{i-1}\alpha_k\right). \tag{36}$$

In both cases: χ_j is given by (32) after it has been rewritten as expressed

$$\begin{bmatrix} \chi_j \overset{\Delta}{=} \alpha_j - R_j^{**}\sum\limits_{k=i}^{j-1}\alpha_k \\ \chi_j \overset{\wedge}{=} \alpha_i \end{bmatrix} \tag{37}$$

Remark 2: The presented results of the studies [23] and [24] have firmly contributed to the role of NOMA system over the Rayleigh fading channels. However, studies on the NOMAn system over the Nakagami-m fading channels have received little attention because of its complexity. Therefore, we investigate the outage probability of each UE over Nakagami-m fading channels with $m = 2$ on both $N-1$ HD/FD relaying nodes. And, the (33) can be solved by applying the PDF in (27) which is expressed in closed-form, respectively, as this research contributions

$$\aleph\Theta_i^{HD,m=2} = \underbrace{\left(1 - \underbrace{\prod_{l=1}^{i-1}\left[e^{-\frac{2R_i^{**}}{\psi_i\rho_{l-1}\sigma_{l-1,l}^2}}\frac{2R_i^{**} + \psi_i\rho_{l-1}\sigma_{l-1,l}^2}{\psi_i\rho_{l-1}\sigma_{l-1,l}^2}\right]}_{\eta}\right)}_{C_1}$$
$$\underbrace{\left(1 - \underbrace{\prod_{j=N}^{i}\left[e^{-\frac{2R_j^{**}}{\chi_j\rho_{i-1}\sigma_{i-1,i}^2}}\frac{2R_j^{**} + \chi_j\rho_{i-1}\sigma_{i-1,i}^2}{\chi_j\rho_{i-1}\sigma_{i-1,i}^2}\right]}_{\mu}\right)}_{C_2}, \tag{38}$$

and

$$\aleph\Theta_i^{FD,m=2} = \underbrace{\left(1 - \underbrace{\prod_{l=1}^{i-1} \left[e^{-\frac{2R_i^{**}}{\psi_i\rho_{l-1}\sigma_{l-1,l}^2}} \frac{\psi_i\rho_{l-1}\sigma_{l-1,l}^2\left(\psi_i\rho_{l-1}\sigma_{l-1,l}^2\left(\psi_i\rho_{l-1}\sigma_{l-1,l}^2+2R_i^{**}\right)+\rho_l\sigma_{LI,l}^2R_i^{**}\left(3\psi_i\rho_{l-1}\sigma_{l-1,l}^2+2R_i^{**}\right)\right)}{\left(\psi_i\rho_{l-1}\sigma_{l-1,l}^2+\rho_l\sigma_{LI,l}^2R_i^{**}\right)^3}\right]}_{\eta}\right)}_{D_1}}{\underbrace{\left(1 - \underbrace{\prod_{j=N}^{i} \left[e^{-\frac{2R_i^{**}}{\chi_j\rho_{i-1}\sigma_{i-1,i}^2}} \frac{\chi_j\rho_{i-1}\sigma_{i-1,i}^2\left(\chi_j\rho_{i-1}\sigma_{i-1,i}^2\left(\chi_j\rho_{i-1}\sigma_{i-1,i}^2+2R_j^{**}\right)+\rho_i\sigma_{LI,i}^2R_j^{**}\left(3\chi_j\rho_{i-1}\sigma_{i-1,i}^2+2R_j^{**}\right)\right)}{\left(\chi_j\rho_{i-1}\sigma_{i-1,i}^2+\rho_i\sigma_{LI,i}^2R_j^{**}\right)^3}\right]}_{\mu}\right)}_{D_2}} \quad (39)$$

There are two cases as described above. It is not necessary to present these cases again. The analysis results will be presented in next section. See appendix for proofing.

3.2. System Throughput

The achievable received data at UE_i, which is also called system throughput P_{sum}^{Ω}, is sum of throughput results of all UEs in system showed by

$$P_{sum}^{\Omega} = \sum_{i=1}^{N} P_i^{\Omega} = \sum_{i=1}^{N} \left(1 - \Theta_i^{\Omega}\right) R_i^* \quad (40)$$

3.3. A Proposed for Energy Harvesting

Proposed 2: In (18) and (19), the received signals at UE_i, with $i > 1$, include two parts which are x_k data symbol and $x_{\varnothing}$ empty symbol where $k = \{i, N\}$ and $l = \{1, i-1\}$. The $x_{\varnothing}$ does not contain information. Therefore, we proposed collecting the energy of allocating power coefficient of the $x_{\varnothing}$ symbol for charging the battery. Another assumption is that the battery is not limited by capacity. Thus, the energy harvesting for each UE in both HD and FD scenarios are expressed by, respectively

$$EH_i = \xi \sqrt{\sum_{l=1}^{i-1} \alpha_l \rho_{i-1} |h_{i-1,i}|^2}, \quad (41)$$

where $i = \{2, N\}$ and ξ is collection coefficient.

3.4. A propose an algorithm for N-1 relaying nodes

Proposed 3: In this section, we propose an algorithm for processing with $N-1$ relaying nodes as showed in Fig. 1. The treatment flow is done in the waterfall pattern in the order showed in Fig. 2.

1. Generate a random N UEs in the network with N channels from BS to UEs.
2. Creating a list of channels in descending order with the element at the top of the list is the best channel. Upon completion of the arrangement, BS will know which user is best chosen to use for first hop relaying node.

3. Through the results of the analysis [23], the authors have found that the performance of the NOMA system depends on the efficiency of the power allocation and the selection of the threshold speed accordingly. Lack of channel state information (CSI) may affect the performance of the NOMA system. We have assumed that at BS and each UE has full CSI of the other UEs. Based on ordering of SCI as showing in (3), we Allocate the power coefficients and select the bit rate threshold for the UEs as, respectively

$$\alpha_i = \frac{\min\left(\sigma_{0,j}^2\right)}{\sum_{k=i}^{N} \sigma_{0,k}^2}, \tag{42}$$

where $i = \{1, N\}$, $j = \{N, 1\}$, and

$$R_i^* = \frac{\max\left(\sigma_{0,i}^2\right)}{\sum_{k=i}^{N} \sigma_{0,k}^2}, \tag{43}$$

where $i = \{1, N\}$. After the BS distributes the transmit power factor to the UEs, logically, a superposed signal is sent to the nearest UE which is selected as the first hop relaying node, namely UE_1.

4. UE_1 receives and decodes x_j symbol with $j = \{N, i\}$ by (20a)-(21b), and excess power is collected by the UE for recharging. The UE_1 will select a next relay node by (23) and send a superposed signal as (18) or (19) to next hop relaying node after UE_1 detects its own symbol, namely x_1, successfully. This work (step 4) will be repeated until the superposed signal will be transmitted to the last UE, namely UE_N in model. The outage probability will occurrence when x_j, where $j = \{N, i\}$, can not be detected successfully at UE_i with $i = \{1, N\}$.

4. Numerical Results and Discussion

It is important to announce that all of our analysis results are simulated by the Matlab software and are presented in most accurate and clearly. We undertake no reproduction of any prior research results. In addition, in this study not using any given data set. In addition, this study does not using any given data set, channels were generated randomly during the simulation of a rule. e.g., if there are random N users, the random channels are arranged according to the rule $|h_{0,1}| > |h_{0,2}| > ... > |h_{0,i}| > ... > |h_{0,N-1}| > |h_{0,N}|$ and the corresponding channel coefficients $1/1 > 1/2 > ... > 1/i > ... > 1/(N-1) > 1/N$

For the results to be clear and accurate, we have performed the Monte Carlo simulation with $1e6$ random samples of each $h_{a,b}$'s channels.

4.1. Numerical Results and Discussion for Outage Probability

It is important to notice that the outage probability results of Direct, HD and FD scenarios are presented by black dashed lines, red dash-dot lines, and blue solid lines, respectively, as showed in Fig. 3(a) and 3(b). In the first case, we assume that there are only three users connected in the network at (t)*th* time slot. We analyzed the performance of the system based on the outage probability of each user in three different scenarios such as Direct, HD and FD schemes. There have some simulation parameters, e.g., the channel coefficients $h_{0,1} = 1$, $h_{0,2} = 1/2$, and $h_{0,3} = 1/3$ are in accordance with the earlier presented assumptions. Based on the transmission channel coefficients of the users, we can allocate power factors for users UE_1, UE_2, and UE_3 with $\alpha_1 = 0.1818$, $\alpha_2 = 0.2727$, $\alpha_3 = 0.5455$, respectively, with $\sum_{i=1}^{3} \alpha_i = 1$ by applying (42). Because the third user, namely UE_3 has the poorest signal quality, it is prioritized to allocate the biggest power factor among the users. Our analysis results showed that users who are far from BS with poor signal quality have better results, e.g., the outage

probability results of the UE_2 and the UE_3 are better than the UE_1, although their signal quality are weaker than the first one. In addition, the Fig. 3(a) showed that UE_3 has the outage probability results which were marked with diamond marker, are best results compared to the other ones, although U_3 has the weakest signal quality $h_{0,3} = 1/3$. Because UE_3 receives more collaboration from the other UEs, the UE_3's QoS has improved. This result demonstrates the effectiveness of our MPCR model. And, the outage probability results of the first user, namely UE_1, has worse results than the other UEs, they are the same in all three scenarios, namely Dir, HD and FD relaying scenarios. The UE_1 with the strongest channel coefficient $h_{0,1} = 1$ has the worst allocation power coefficient $\alpha_1 = 0.1818$ compared to the others. A previous study of FD relaying in [27] and the results of comparison between FD and HD in [28] showed that the outage probability the relaying in FD mode was worse than HD one. There is a similarity in this research results. The system performance efficiency of the MPCR model with $N-1$ FD relaying nodes has resulted in approximation with $N-1$ HD relaying nodes in the low dB SNRs. But as the SNRs ascending, the performance of the MPCR system with N-1 HD relaying nodes becomes better demonstrated by the red dash-dot lines in Fig. 3.(a). Specially, although the first user's outage probability results in the FD scenario are the worst, there are not much difference compared to the other scenarios, such as direct and HD scenarios. This is because the first relaying node in FD mode is affected by its own antenna channel noise, whereas in the direct and HD transmission scenarios with one antenna have no interference channels.

UEs	Channels	Allocation power coefficents	Bit rate thresholds
UE_1	$h_{0,1} = 1$	$\alpha_1 = 0.1818$	$R_1^* = 0.5455$
UE_2	$h_{0,2} = 0.5$	$\alpha_2 = 0.2727$	$R_2^* = 0.2727$
UE_3	$h_{0,3} = 0.3333$	$\alpha_3 = 0.5455$	$R_3^* = 0.1818$

Table 1. 3 UEs in NOMA system (t)th time slot.

To be more clearer, we increased the number of users in the network to $N = 4$ users with the channel coefficient of UE_4 was $h_{0,4} = 1/4$ at (t+1) time slot. And, the outage probability of the users are presented in Fig. 3(b). Because the system has a new joined user, namely UE_4, involved in the network with very weak signal quality. Therefore, we reused (42) to reallocate the transmit power factors to the users with $\alpha_1 = 0.12$, $\alpha_2 = 0.16$, $\alpha_3 = 0.24$, $\alpha_4 = 0.48$ as showed in table 2. And because the power distribution coefficients have been changed. As a result, the instantaneous bit rate thresholds of users are also have been changed accordingly. The instantaneous bit rate thresholds of the user are $R_i^* = \{0.48, 0.24, 0.16, 0.12\}$ with $i = \{1, 4\}$. In this case, to ensure the QoS to the fourth user with the poorest signal quality, we have allocated to this user the biggest power factor, namely $\alpha_4 = 0.48$, and the lowest threshold, namely $R_4^* = 0.12$, compared with other users in the network. In addition, the other users must share power coefficient to UE_4 in power domain. The compared row contents in table 1 and table 2 correspondingly, both α_i and R_i^* with $i = \{1, 3\}$ are reduced for sharing power and bit rate to UE_4. As showed in Fig. 3(b), although the UE_4 has the poorest signal quality, but it has the best outage probability results. This demonstrates that the MPCR combines with allocation power factor method and the instantaneous bit rate threshold selection method are effective. In particular, the outage probability results in both HD and FD scenarios using N-1 relaying nodes always outperform scheme with no relaying.

Furthermore, we analyze the impact of both allocation power coefficient and SNRs affect user's service quality, especially weak users. In Fig. 3(b), the weakest user UE_4 has been assigned a fixed power factor $\alpha_4 = 0.48$. I consider if the power allocation coefficient for UE_4 increases or decreases, the quality of service of UE_4 is varied over the corresponding SNRs. For simplicity, we assume that

Preprints (www.preprints.org) | NOT PEER-REVIEWED | Posted: 10 December 2018 doi:10.20944/preprints201812.0109.v1

Peer-reviewed version available at Electronics 2019, 8, 167; doi:10.3390/electronics8020167

UEs	Channels	Allocation power coefficents	Bit rate thresholds
UE_1	$h_{0,1} = 1$	$\alpha_1 = 0.1200$	$R_1^* = 0.4800$
UE_2	$h_{0,2} = 0.5$	$\alpha_2 = 01600$	$R_2^* = 0.2400$
UE_3	$h_{0,3} = 0.3333$	$\alpha_3 = 0.2400$	$R_3^* = 0.1600$
UE_4	$h_{0,4} = 0.2500$	$\alpha_4 = 0.4800$	$R_4^* = 0.1200$

Table 2. 4 UEs in NOMA system at (t+1)th time slot.

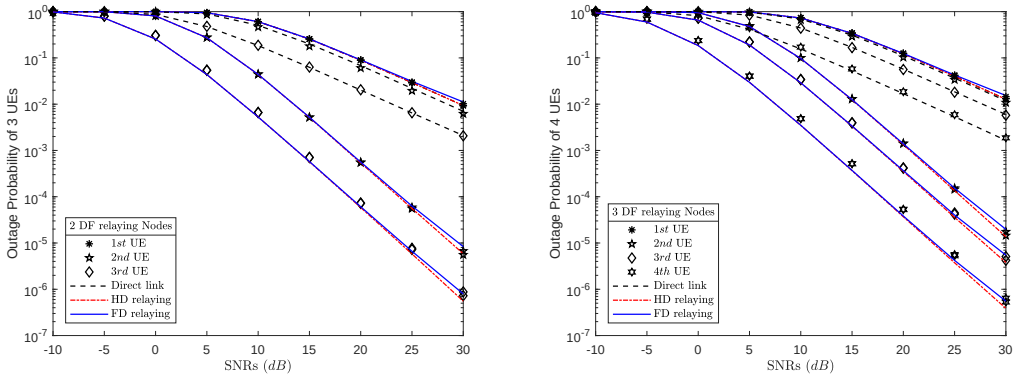

(a) 2 DF relaying nodes. (b) 3 DF relaying nodes.

Figure 3. The outage probability results of $N = \{3, 4\}$ UEs over Rayleigh fading channels.

user UE_4 is over the Rayleigh fading channel. And, the users are over Nakagami-m fading channels will be analyzed later. The Fig. 4 showed the outage probability of the UE_4 with the allocation power factor which can be variable. We have assumed that the fourth user can be allocated a variable power factor $\|\alpha_4\| = \{0.1, 0.9\}$ instead of fixing $\alpha_4 = 0.48$ as Fig. 3(b). By one-by-one submitting each value $\|\alpha_4\|$ into (34), (35), (38), and (39). It is important to notice that the outage probability results of UE_4 in direct, HD relaying, FD relaying scenario are presented by solid grid, dashed grid, and dash-dot grid. The Fig. The 4 showed that the outage probability results of UE_4 in HD relaying and FD relaying scenarios are better than the UE_4's results in direct scenario. Specially, the outage probability results of UE_i in MPCR system with $N - 1$ HD/FD relaying nodes are also approximations in all SNRs. This result is consistent with the results presented earlier in Fig. 3(a) and 3(b).

In addition, we investigate outage probability of users over Nakagami-m fading channels scenario versus the ones over Rayleigh fading channels scenario as showing in Fig. 5. To ensure that this comparison is fair, the simulation parameters in the Nakagami-m fading channles scenario are the same as the simulation parameters showed in table 1. Therefore, it is not necessary to present these simulation parameters again. In low SNRs, the outage probability results of the users over Rayleigh fading channels and Nakagami-m fading channels are approximated. However, when the SNRs are increased, the outage probability results of the user over the Nakagami-m scenario are greatly improved.

4.2. Numerical Results and Discussion for System Throughput

In system performance evaluation, system throughput is an important criterion that is known as the sum of instantaneous achievable bit rate of each user in the system. We reuse the simulation parameters as described in the evaluation of the outage probability showed in table 1 and table 2. Therefore, we do not restate these parameters. The system throughput of each user with $N = 3$ UEs and $N = 4$ ones are presented in Fig. 6(a) and 6(b), respectively. It is important to notice that the solid lines, dash-dot lines and dashed lines are the system throughput of the users in direct, HD and FD scenarios, respectively. Because the outage probability of the users in HD and FD scenarios are approximately equal. As a result, the throughput results of these users are also approximately equal.

Preprints (www.preprints.org) | NOT PEER-REVIEWED | Posted: 10 December 2018 doi:10.20944/preprints201812.0109.v1

Peer-reviewed version available at Electronics 2019, 8, 167; doi:10.3390/electronics8020167

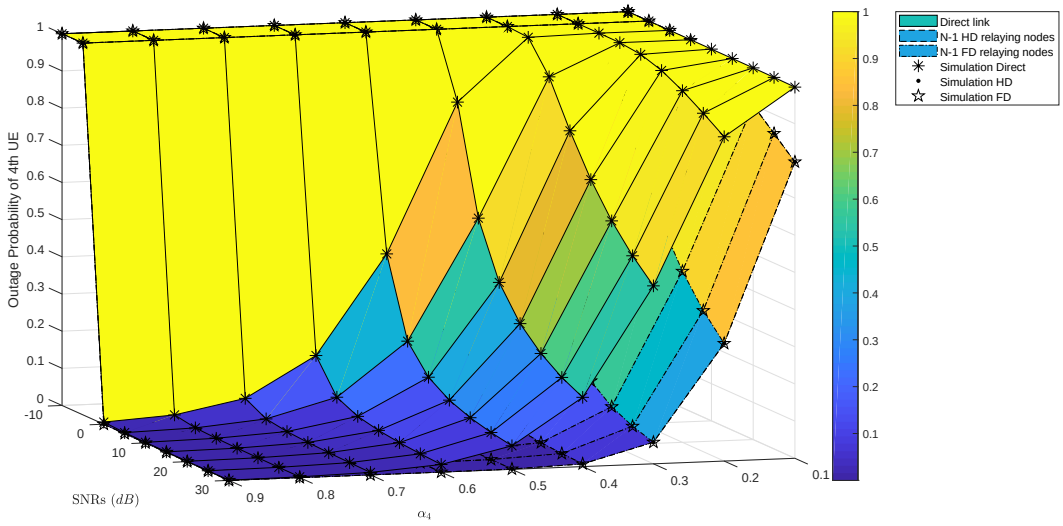

Figure 4. The outage probability results of $4th$ UE with $\|\alpha_4\| = \{0.1, 0.9\}$ and $SNRs = \{-10, 30\}$.

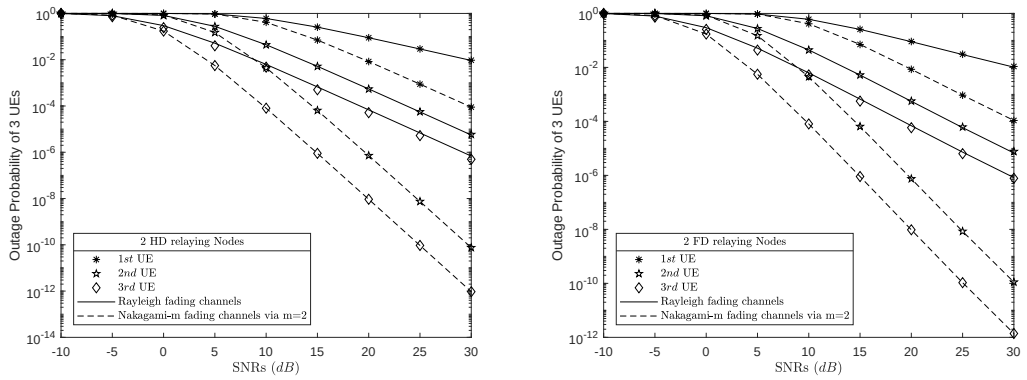

(a) 2 HD relaying nodes.

(b) 2 FD relaying nodes.

Figure 5. The outage probability results of 3 UEs over Rayleigh fading channels versus Nakagami-m fading channels via $m = 2$

Thus, the dash-dot lines and dashed ones are overlapped in both Fig. 6(a) and 6(b). The analysis results showed that the system throughput of users in the $N-1$ HD/FD relaying nodes scenarios are always better than the system throughput of the ones in the non-relay scenario. Specifically, the first UE's system throughput is approximate in all three scenarios. At SNR in 30 dB, all users in three scenarios reach their bit rate thresholds R_i^*.

On another hand, We analyze the impact of the allocation power factor α_4 on the fourth user's throughput with variable $\|\alpha_4\| = \{0.1, 0.9\}$ values instead fixing it $\alpha_4 = 0.48$. As showing in Fig. 7, higher grid lines are better results than the ones. In this case, the instantaneous bit rate threshold of UE_4 is $R_4^* = 0.12$ bps/Hz. In low SNRs, e.g. $SNR = 0$ db, the system throughput results in all scenarios are approximately zero. On another hand, although the SNR has increased, e.g. $SNR = 10$ dB, the system throughput results are still approximately zero if the power factor, namely α_4 is still in low, e.g. $\alpha_4 = 0.1$. But with $\alpha_4 = 0.4$ though SNR is still held at 10 dB, the system throughput results of UE_4 in both HD and FD scenarios are improved and reach their bit rate threshold. And, in Fig. 6(a) showed that at SNR in 10 dB and $\alpha_4 = 0.48$, the UE_4 reach its bit rate threshold, approximately.

Preprints (www.preprints.org) | NOT PEER-REVIEWED | Posted: 10 December 2018 doi:10.20944/preprints201812.0109.v1

Peer-reviewed version available at Electronics 2019, 8, 167; doi:10.3390/electronics8020167

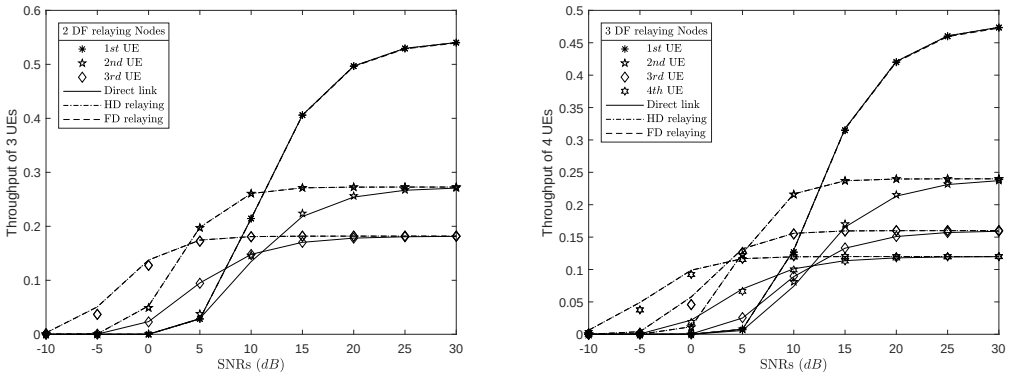

(a) $N = 3$ UEs in network. (b) $N = 4$ UEs in network.

Figure 6. The system throughput results of the users over Rayleigh fading channels.

Another e.g., in paired $\alpha_4 = 0.5$ and $SNR = 0$ dB, UE_4 also reach its bit rate threshold. By this analysis, we can find pairs of values α_4 and SNR where UE_4 can reach the threshold $R_4^* = 0.12$ bps/Hz.

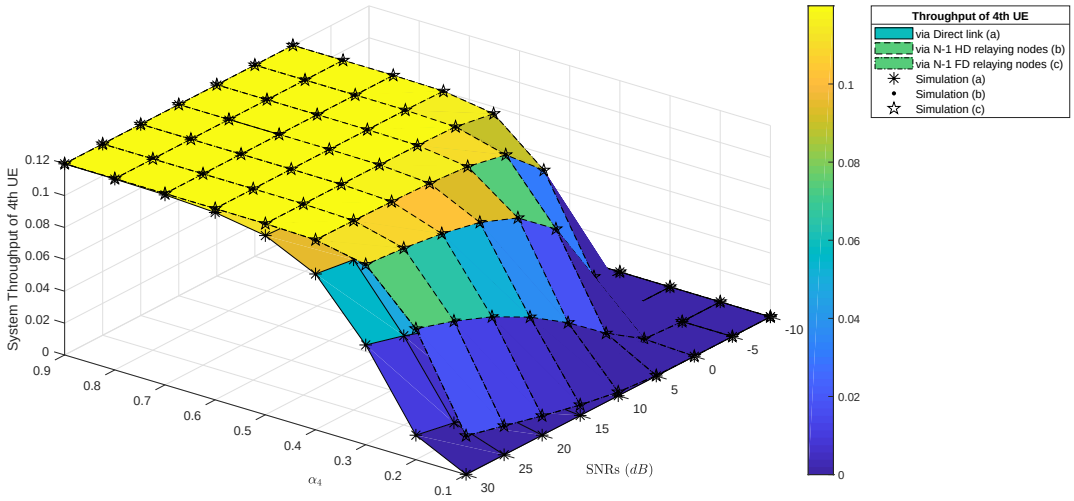

Figure 7. The throughput of the $4th$ UE over Rayleigh fading channels with $\|\alpha_4\| = \{0.1, 0.9\}$ and $SNRs = \{-10, 30\}$.

The system throughput of the users in $N-1$ HD relaying nodes over both Rayleigh and Nakagami-m scenarios were analyzed, compared and presented in Fig. 8(a). In Fig. 8(a), There are $N = 3$ UEs over Rayleigh fading channels and Nakagami-m fading channels with solid lines and dashed ones, respectively. Because $\Theta_1^{HD} > \Theta_2^{HD} > \Theta_3^{HD}$ as showing in Fig. 5(a). By applying (40), we get $P_1^{HD} < P_2^{HD} < P_3^{HD}$ with low SNRs. But as the SNR increases, the system throughput of each UE changes, e.g. $SNR = 30$ dB, $P_1^{HD} > P_2^{HD} > P_3^{HD}$ and reach their bit rate thresholds R_i^*.

The similarly results happen in $N-1$ FD relaying nodes scheme as showing in Fig. 8(b). Specially, because the users over Nagami-m fading channels have better outage probability results than the ones over the Rayleigh fading channels as showing in Fig. 5(b), in some SNRs, e.g., $SNR = 10$ dB then $\aleph\Theta_i^{FD} < \Re\Theta_i^{FD}$. Therefore, $\aleph P_i^{FD} > \Re P_i^{FD}$ where $\aleph$ and $\Re$ were denoted as Nakagami-m and Rayleigh fading channels, respectively, after we applied (40). these results proved that the Nakagami-m channel

Preprints (www.preprints.org) | NOT PEER-REVIEWED | Posted: 10 December 2018 doi:10.20944/preprints201812.0109.v1

Peer-reviewed version available at Electronics 2019, 8, 167; doi:10.3390/electronics8020167

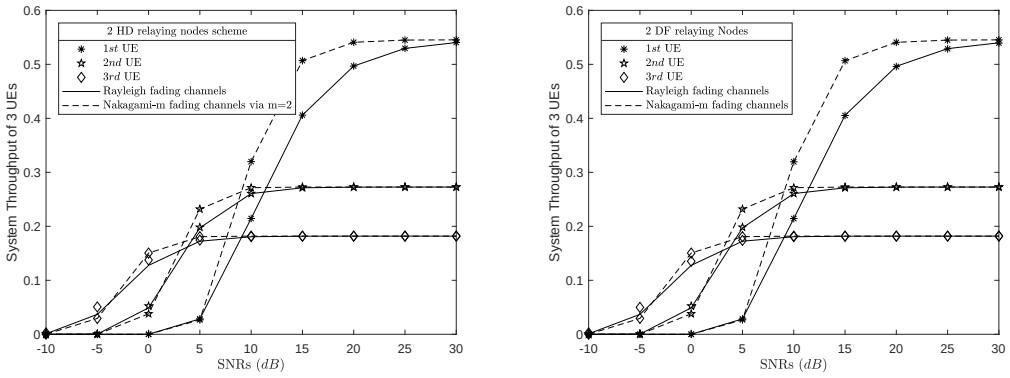

(a) N-1 HD relaying nodes. (b) N-1 FD relaying nodes.

Figure 8. Compared the system throughput results of Rayleigh versus Nakagami-m via m=2.

is better than the Rayleigh channel. However, when we are increasing SNRs, there have approximately the same results and close to the thresholds $\aleph P_i^{HD} \approx \Re P_i^{HD} \approx R_i^*$.

4.3. N UEs with N-1 HD/FD Relaying Nodes

As models in Fig. 1(a) and (b), the proposed algorithm 1 can investigate the system performance with N UEs where N is a random and big number. Because of the limited power of our personal computers, we only analyze and present cases where there are only 3 or 4 users in the system. But the results presented do not show all the advantages of our algorithm. Thus, we are increasing limit the number user with bigger number N. As Fig. 9(a) and (b), there have 9 UEs in the network. By applying algorithm 1, we investigated the outage probability of the UEs in the network over both Rayleigh and Nakagami-m fading channels. For e.g., in $N-1$ HD relaying nodes scenario, the outage probability of the first UE, namely UE_1, can be calculated by (34) or (28) over Rayleigh or Nakagami-m fading channels with $m = 2$, respectively, where $\eta = 0$. Another e.g., in FD scenario, the outage probability of last UEs, namely UE_9, over Rayleigh or Nakamagmi-m fading channels can be computed by (35) or (39), respectively. With the number of users is greater than 9, the results of the analysis are difficult to observe in the figure and it need more time for the simulation so we end our analysis with up to 9 users in network.

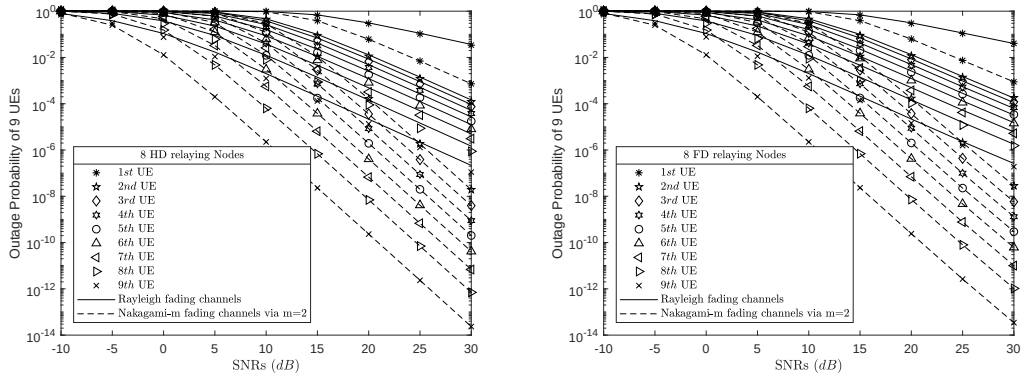

(a) 9 UEs in 8 HD relaying nodes model. (b) 9 UEs in 8 FD relaying nodes model.

Figure 9. Compared the outage probability results of Rayleigh versus Nakagami-m fading channels

5. Conclusion

In this study, we proposed a novel NOMA network model with $N-1$ relaying nodes instead of using only one relay as previous studies. A superposed signal would be sent through $N-1$ relaying nodes before it reaches the farthest UE which is denoted by UE_N. The closed-form expressions of $N-1$ HD/FD relaying nodes scenarios over Rayleigh/Nakagami-m fading channels are also presented along with an explanation for the corresponding processing. By presenting results in the figures, our proposed models with $N-1$ HD/FD relaying nodes are effective for applying to the cooperator NOMA network in next generation wireless telecommunications.

Author Contributions:

T-NT is the first author who has proposed the main idea, analyzed and simulated the system, and presented the writing—original draft preparation, writing—review and editing, visualization.

MV are the second and third authors who has experiences in wireless communication research. They have made a supervision, review, given the first author some useful comments and funding acquisition for this research.

All authors read and approved the final manuscript.

Funding: This research received no external funding.

Acknowledgments: N/A

Conflicts of Interest: We declare no conflict of interest. The funders had no role in the design of the study; in the collection, analyses, or interpretation of data; in the writing of the manuscript, or in the decision to publish the results.

Abbreviations

The following abbreviations are used in this manuscript:

No.	Abbreviations	Full description
1	AWGNs	Additive white Gaussian noises
2	BS	Base station
3	CDF	Cummuative distribution function
4	CSI	Channel state information
5	Fig.	Figure
6	NOMA	non-orthogonal multiple access
7	OFDMA	Orthogonal frequency-division multiple access
8	PDF	Probability density function
9	QoS	Quality of service
10	S	Source
11	SIC	Successive interference cancellation
12	SINR	Signal-to-interference-plus-noise ratio
13	SNR	Signal-to-noise ratio
14	UEs	User Equipments

Table 3. The abbreviations table.

Proof of $N-1$ HD relaying nodes scenario: The condition for occurrence of the outage events has been presented in (33). By submitting (22), where $\Omega = HD$, into (33), we can get a expression for computing the outage probability of each UE in $N-1$ HD relaying nodes scenario.

$$\Theta_i^{HD} = \left(1 - \prod_{l=1}^{i-1} \Pr\left(|h_{l-1,l}|^2 > \frac{R_i^{**}}{\chi_i \rho_{l-1}}\right)\right) and \left(1 - \prod_{j=N}^{i} \Pr\left(|h_{i-1,i}|^2 > \frac{R_j^{**}}{\chi_j \rho_{i-1}}\right)\right) \quad \text{(A1)}$$

The (A1) can be rewritten in experimental integral by applying the PDF (25) of Rayleigh distributions as

$$\Re\Theta_i^{HD} = \left(1 - \prod_{l=1}^{i-1} \int_{\frac{R_i^{**}}{\chi_i \rho_{l-1}}}^{\infty} \frac{1}{\sigma_{l-1,l}^2} e^{-\frac{x}{\sigma_{l-1,l}^2}} dx\right) and \left(1 - \prod_{j=N}^{i} \int_{\frac{R_j^{**}}{\chi_j \rho_{i-1}}}^{\infty} \frac{1}{\sigma_{i-1,i}^2} e^{-\frac{x}{\sigma_{i-1,i}^2}} dx\right). \quad \text{(A2)}$$

The (A2) can be solved and expressed as (34).
On another hand, the (A2) can be written with the PDF (27) of Nakagami-m fading channels as

$$\aleph\Theta_i^{HD} = \left(1 - \prod_{l=1}^{i-1} \int_{\frac{R_i^{**}}{\chi_i \rho_{l-1}}}^{\infty} \left(\frac{m}{\sigma_{l-1,l}^2}\right)^m \frac{x^{m-1}}{\Gamma(m)} e^{-\frac{mx}{\sigma_{l-1,l}^2}} dx\right) and \left(1 - \prod_{j=N}^{i} \int_{\frac{R_j^{**}}{\chi_j \rho_{i-1}}}^{\infty} \left(\frac{1}{\sigma_{i-1,i}^2}\right)^m \frac{x^{m-1}}{\Gamma(m)} e^{-\frac{mx}{\sigma_{i-1,i}^2}} dx\right) \quad \text{(A3)}$$

and after the (A3) was solved, it can be expressed as (38). □

Proof of $N-1$ FD relaying nodes scenario: In similarly, by submitting (**??**), where $\Omega = FD$, into (33), we can get a expression for computing the outage probability of each UE in $N-1$ FD relaying nodes scenario.

$$\Theta_i^{FD} = \left(1 - \prod_{l=1}^{i-1} \Pr\left(|h_{l-1,l}|^2 > \frac{R_i^{**}\left(|h_{Li,l}|^2 \rho_l + 1\right)}{\chi_i \rho_{l-1}}, |h_{Li,l}|^2 > 0\right)\right) \quad \text{(A4)}$$
$$\left(1 - \prod_{j=N}^{i} \Pr\left(|h_{i-1,i}|^2 > \frac{R_j^{**}\left(|h_{Li,i}|^2 \rho_i + 1\right)}{\chi_j \rho_{i-1}}, |h_{Li,i}|^2 > 0\right)\right)$$

The (A4) is also rewritten in experimental integral by applying the PDF of Rayleigh or Nakagami-m fading which are respectively (25) or (27), respectively, as

$$\Re\Theta_i^{HD} = \left(1 - \prod_{l=1}^{i-1} \int_0^{\infty} \int_{\frac{R_i^{**}(y\rho_l+1)}{\chi_i \rho_{l-1}}}^{\infty} \frac{1}{\sigma_{l-1,l}^2 \sigma_{LI,l}^2} e^{-\left(\frac{x}{\sigma_{l-1,l}^2} + \frac{y}{\sigma_{LI,l}^2}\right)} dxdy\right) \quad \text{(A5)}$$
$$\left(1 - \prod_{j=N}^{i} \int_0^{\infty} \int_{\frac{R_j^{**}(y\rho_i+1)}{\chi_j \rho_{i-1}}}^{\infty} \frac{1}{\sigma_{i-1,i}^2 \sigma_{LI,i}^2} e^{-\left(\frac{x}{\sigma_{i-1,i}^2} + \frac{y}{\sigma_{LI,i}^2}\right)} dxdy\right).$$

and

$$\aleph\Theta_i^{FD} = \left(1 - \prod_{l=1}^{i-1} \int_0^{\infty} \int_{\frac{R_i^{**}(y\rho_l+1)}{\chi_i\rho_{l-1}}}^{\infty} \left(\frac{m^2}{\sigma_{l-1,l}^2\sigma_{LI,l}^2}\right)^m \frac{(xy)^{m-1}}{(\Gamma(m))^2} e^{-m\left(\frac{x}{\sigma_{l-1,l}^2}+\frac{y}{\sigma_{LI,l}^2}\right)} dxdy\right) \left(1 - \prod_{j=N}^{i} \int_0^{\infty} \int_{\frac{R_j^{**}(y\rho_i+1)}{\chi_j\rho_{i-1}}}^{\infty} \left(\frac{m^2}{\sigma_{i-1,i}^2\sigma_{LI,i}^2}\right)^m \frac{(xy)^{m-1}}{(\Gamma(m))^2} e^{-m\left(\frac{x}{\sigma_{i-1,i}^2}+\frac{y}{\sigma_{LI,i}^2}\right)} dxdy\right) \quad \text{(A6)}$$

For e.g. $m = 2$, the (A5) and (A6) are solved and expressed as (38) and (39), respectively. End of proof. □

References

1. Y. Saito, A. Benjebbour, Y. Kishiyama and T. Nakamura, "System-level performance evaluation of downlink non-orthogonal multiple access (NOMA)", 2013 IEEE 24th Annual International Symposium on Personal, Indoor, and Mobile Radio Communications (PIMRC), 2013.
2. Z. Ding, Z. Yang, P. Fan and H. Poor, "On the Performance of Non-Orthogonal Multiple Access in 5G Systems with Randomly Deployed Users", IEEE Signal Processing Letters, vol. 21, no. 12, pp. 1501-1505, 2014.
3. Y. Lan, A. Benjebboiu, X. Chen, A. Li and H. Jiang, "Considerations on downlink non-orthogonal multiple access (NOMA) combined with closed-loop SU-MIMO", 2014 8th International Conference on Signal Processing and Communication Systems (ICSPCS), 2014.
4. Z. Ding, M. Peng and H. Poor, "Cooperative Non-Orthogonal Multiple Access in 5G Systems", IEEE Communications Letters, vol. 19, no. 8, pp. 1462-1465, 2015.
5. Y. Xiao, L. Hao, Z. Ma, Z. Ding, Z. Zhang and P. Fan, "Forwarding Strategy Selection in Dual-Hop NOMA Relaying Systems", IEEE Communications Letters, vol. 22, no. 8, pp. 1644-1647, 2018.
6. A. Davoodi, M. Emadi and M. Aref, "Analytical power allocation for a full duplex decode-and-forward relay channel", 2013 Iran Workshop on Communication and Information Theory, 2013.
7. Z. Ding, H. Dai and H. Poor, "Relay Selection for Cooperative NOMA", IEEE Wireless Communications Letters, vol. 5, no. 4, pp. 416-419, 2016.
8. H. Gao, W. Ejaz and M. Jo, "Cooperative Wireless Energy Harvesting and Spectrum Sharing in 5G Networks", IEEE Access, vol. 4, pp. 3647-3658, 2016.
9. A. Tonello, F. Versolatto and S. D'Alessandro, "Opportunistic Relaying in In-Home PLC Networks", 2010 IEEE Global Telecommunications Conference GLOBECOM 2010, 2010.
10. L. Lampe and A. Vinck, "Cooperative multihop power line communications," IEEE Int. Symp. Power Line Commun. and Its Appl. (ISPLC), pp. 1–6, Mar. 2012.
11. X. Cheng, R. Cao, and L. Yang, "Relay-aided amplify-and-forward powerline communications," IEEE Trans. Smart Grid, vol. 4, pp. 265–272, Mar. 2013.
12. K. Rabie, B. Adebisi, H. Gacanin, G. Nauryzbayev and A. Ikpehai, "Performance evaluation of multi-hop relaying over non-gaussian PLC channels", Journal of Communications and Networks, vol. 19, no. 5, pp. 531-538, 2017.
13. A. Dubey, R. K. Mallik, and R. Schober, "Performance analysis of a multi-hop power line communication system over log-normal fading in presence of impulsive noise," IET Commun., vol. 9, no. 1, pp. 1–9, 2015.
14. A. Dubey and R. K. Mallik, "PLC system performance with AF relaying," IEEE Trans. Commun., vol. 63, pp. 2337–2345, Jun. 2015.
15. Z. Ding, H. Dai and H. Poor, "Relay Selection for Cooperative NOMA", IEEE Wireless Communications Letters, vol. 5, no. 4, pp. 416-419, 2016.
16. X. Lu, P. Wang, D. Niyato, D. I. Kim, and Z. Han, "Wireless networks with RF energy harvesting: A contemporary survey," IEEE Commun. Surveys Tuts., vol. 17, pp. 757–789, 2015.

17. A. A. Nasir, H. D. Tuan, D. T. Ngo, S. Durrani, and D. I. Kim, "Path-following algorithms for beamforming and signal splitting in RF energy harvesting networks," IEEE Commun. Letters, vol. 20, no. 8, pp. 1687–1690, Aug 2016.
18. V. D. Nguyen, T. Q. Duong, H. D. Tuan, O. S. Shin, and H. V. Poor, "Spectral and energy efficiencies in full-duplex wireless information and power transfer," IEEE Trans. Commun., vol. 65, no. 5, pp. 2220–2233, May 2017.
19. H. H. M. Tam, H. D. Tuan, A. A. Nasir, T. Q. Duong, and H. V. Poor, "MIMO energy harvesting in full-duplex multi-user networks," IEEE Trans. Wirel. Commun., vol. 16, no. 5, pp. 3282–3297, May 2017.
20. A. A. Nasir, H. D. Tuan, T. Q. Duong, and H. V. Poor, "Secrecy rate beamforming for multicell networks with information and energy harvesting," IEEE Trans. Signal Process., vol. 65, no. 3, pp. 677–689, 2017.
21. K. HIGUCHI and A. BENJEBBOUR, "Non-orthogonal Multiple Access (NOMA) with Successive Interference Cancellation for Future Radio Access", IEICE Transactions on Communications, vol. 98, no. 3, pp. 403-414, 2015.
22. Y. Jing and H. Jafarkhani, "Single and multiple relay selection schemes and their achievable diversity orders," IEEE Transactions on Wireless Communications, vol. 8, no. 3, pp. 1414–1423, Mar. 2009.
23. Ding, H. Dai and H. Poor, "Relay Selection for Cooperative NOMA", IEEE Wireless Communications Letters, vol. 5, no. 4, pp. 416-419, 2016.
24. Kim and I. Lee, "Capacity Analysis of Cooperative Relaying Systems Using Non-Orthogonal Multiple Access", IEEE Communications Letters, vol. 19, no. 11, pp. 1949-1952, 2015.
25. A. K. Sadek, Z. Han, and K. J. R. Liu, "A distributed relay-assignment algorithm for cooperative communications in wireless networks," IEEE Int. Conf. Commun., Istanbul, Turkey, June 2006.
26. V. Sreng, H. Yanikomeroglu, and D. D. Falconer, "Relay selection strategies in cellular networks with peer-to-peer relaying," in Proc. IEEE Veh. Technol. Conf., Orlando, FL, Oct. 2003.
27. T. Thanh-Nam, D. Dinh-Thuan, and M. Voznak, "Full-duplex Cognitive Radio NOMA Networks: Outage and Throughput Performance Analysis," in Proc. International Journal of Electronics and Telecommunications, vol. 65, no. 1, 2019.
28. T. Thanh-Nam, D. Dinh-Thuan, and M. Voznak, "On Outage Probability and Throughput Performance of Cognitive Radio Inspired NOMA Relay System," in Proc. Advances in Electrical and Electronic Engineering, 2019.

About the Authors ...

Nam T. TRAN was born in Vinh Long province, Vietnam. He received his M.Sc. from Military Technical Academy (MTA) in 2014. He works in the faculty of Electronics and Telecommunications, Sai Gon University, Ho Chi Minh city, Viet Nam. He is currently pursuing his Ph.D. degree in Electrical Engineering at VSB Technical University of Ostrava, Czech Republic. His major interests are in NOMA, energy harvesting, cognitive radio, and physical layer security.

Miroslav VOZNAK received the Ph.D.degree in telecommunications from the Faculty of Electrical Engineering and Computer Science, VSB-Technical University of Ostrava and completed his habilitation in 2002 and 2009, respectively. He was appointed Full Professor in 2017 in Electronics and Communication technologies. He is an IEEE senior member and he has served as a member of editorial boards for several journals, such as the Journal of Communications or the Advances in Electrical and Electronic Engineering. His research interests focus generally on information and communications technology, particularly on quality of service and experience, network security, wireless networks and in the last couple years also on big data analytics.